

# The role of hot uprising plumes in the initiation of plate-like regime of three-dimensional mantle convection

Masaki Yoshida

Earth Simulator Center, Japan Marine Science and Technology Center, Yokohama, Kanagawa, Japan

Masaki Ogawa

Department of Earth Sciences and Astronomy, University of Tokyo at Komaba, Tokyo, Japan

Received 20 March 2003; revised 20 January 2004; accepted 21 January 2004; published 9 March 2004.

[1] Three-dimensional numerical models are presented for thermal convection of non-Newtonian fluid with viscosity that depends on temperature and stress to understand development of moving plates on the Earth. A hysteresis is assumed in the relationship between stress and viscosity to make the viscosity depend on stress-history. The stress-history dependence due to hysteresis induces a regime where plates or highly viscous pieces of lithosphere separated by narrow and mechanically weak plate margins rigidly move by their own weight. The plate margins newly develop when a stress high enough to cause lithospheric rupture is induced in the lithosphere by the help of hot cylindrical uprising plumes but do not spontaneously develop by the weight of lithosphere itself. The high rupture strength of lithosphere makes the plate-like motion rather steady without the help of viscosity reduction by melting in the asthenosphere. *INDEX TERMS:* 8120 Tectonophysics: Dynamics of lithosphere and mantle—general; 8121 Tectonophysics: Dynamics, convection currents and mantle plumes; 8150 Tectonophysics: Plate boundary—general (3040); 8155 Tectonophysics: Plate motions—general; 8162 Tectonophysics: Rheology—mantle. **Citation:** Yoshida, M., and M. Ogawa (2004), The role of hot uprising plumes in the initiation of plate-like regime of three-dimensional mantle convection, *Geophys. Res. Lett.*, *31*, L05607, doi:10.1029/2003GL017376.

## 1. Introduction

[2] It is one of the major challenges in numerical studies of mantle convection to self-consistently reproduce moving plates in three-dimensional space [e.g., *Bercovici et al.*, 2000]. Plate motion occurs when narrow plate margins as mechanically weak zones develop in a rigid lithosphere. Several candidates have been proposed for the mechanism that induces such narrow plate margins in the Earth's lithosphere; power-law creep [e.g., *Christensen*, 1984], yielding [e.g., *Moresi and Solomatov*, 1998; *Trompert and Hansen*, 1998; *Tackley*, 2000a; *Richards et al.*, 2001], viscous heating [e.g., *Bercovici*, 1996], void-volatile weakening [*Bercovici*, 1998], and strain-rate weakening rheology with damage evolution and time healing (abbreviated as “DETH”) [*Bercovici*, 1998; *Tackley*, 2000b]. Among the candidates, yielding [*Trompert and Hansen*, 1998; *Tackley*, 2000a; *Richards et al.*, 2001] and strain-rate weakening rheology with DETH [*Tackley*, 2000b] have been implemented in three-dimensional numerical models of mantle convection

and have been found to mobilize rigid and stagnant lithosphere by inducing narrow plate margins. The plate-like behavior modeled in this way is, however, strongly time-dependent and the moving plates are not satisfactorily rigid unless viscosity reduction by melting in the asthenosphere is taken into account [*Tackley*, 2000b; *Richards et al.*, 2001]. To understand why the stable tectonic-plates exists on the Earth [e.g., *Bercovici et al.*, 2000], it is important to develop various models of rigidly moving plates both with and without viscosity reduction by melting. Here, we present a three-dimensional numerical model of mantle convection where the plate-like behavior of the lithosphere is induced by a version of DETH mechanism that has been found to induce a very steady motion of rigid plates in two-dimensional space without the help of viscosity reduction by melting [*Ogawa*, 2003].

## 2. Model Description

[3] A thermal convection of an incompressible Newtonian fluid is considered in a three-dimensional, Cartesian, internally heated box with 2900 km in thickness and an aspect ratios of 3. The Prandtl number is infinite and the Boussinesq approximation is employed. All of the boundaries of the vessel are impermeable and shear stress-free, i.e., the reflective condition is applied to the sidewalls. The top surface boundary ( $z = 1$ ) is isothermal, while the side boundaries are adiabatic. For the thermal boundary condition on the bottom boundary ( $z = 0$ ), see below.

[4] The viscosity  $\eta$  depends on temperature  $T$ , depth  $1 - z$  and “damage parameter”  $\omega$  as

$$\eta = \exp \left[ -ET + V(1 - z) - F \frac{\omega}{1 + \omega} \right], \quad (1)$$

[*Ogawa*, 2003], where  $E$ ,  $V$  and  $F$  are constants and are fixed at  $E = \ln(10^{6.0})$ ,  $V = \ln(10^{2.0})$  and  $F = \ln(10^{3.5})$ . The damage parameter evolves with time  $t$  as

$$\frac{\partial \omega}{\partial t} + \mathbf{v} \cdot \nabla \omega = \Gamma \sigma_{ij} \dot{\epsilon}_{ij} - \lambda_0 \exp(ET) \cdot \omega, \quad (2)$$

[*Bercovici*, 1998; *Tackley*, 2000a; *Ogawa*, 2003], where  $\mathbf{v}$  is velocity,  $\sigma_{ij}$  is deviatoric stress,  $\dot{\epsilon}_{ij}$  is strain rate,  $\lambda_0$  is a constant, and  $\Gamma$  is treated as a free parameter (see below). This equation implies that (1) the damaging rate is proportional to viscous dissipation rate as is the case for void-volatile weakening [e.g., *Bercovici*, 1998] (one note

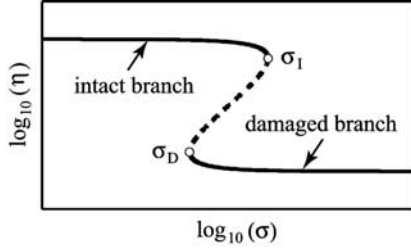


**Figure 1.** The relationship of viscosity versus stress. The convecting fluid selects one of the two branches indicated by the solid parts of the curve, i.e., intact branch or damaged branch, depending on the stress-history that the fluid has experienced in the past. The dashed part of the curve is physically unrealizable (see *Ogawa* [2003] for detail).

that not all deformational work is necessarily associated with viscous dissipation [e.g., *Bercovici et al.*, 2001; *Ricard et al.*, 2001; *Bercovici and Ricard*, 2003]), and (2) the convecting material recovers from damage with a healing time that depends on temperature. The healing time  $1/\lambda_0$  at  $T = 0$  is  $10^{-5}$ . There is no flow of  $\omega$  across any of the boundaries.

[5] Because of the short healing time, the steady state assumption holds well for Equation (2) and the left hand side of Equation (2) is negligible in most cases. Under this assumption, Equations (1) and (2) give a relationship between viscosity and stress illustrated in Figure 1. The critical stress  $\sigma_I$  in the figure is the maximum stress on the “intact branch”, which is characterized by  $\omega \ll 1$  in Equation (1) and corresponds to the rupture strength of plate interior, while  $\sigma_D$  is the minimum stress on the “damaged branch”, which is characterized by  $\omega \gg 1$  and corresponds to the rupture strength of plate margins. The values of  $\sigma_I$  and  $\sigma_D$  are calculated from the parameter values described above and the expression for these quantities shown in *Ogawa* [2003] as

$$\sigma_I = \frac{72.6}{\sqrt{\Gamma}} \quad \text{and} \quad \sigma_D = \frac{24.5}{\sqrt{\Gamma}}. \quad (3)$$

The convecting fluid selects one of the two branches in the stress range from  $\sigma_D$  to  $\sigma_I$  depending on the stress-history that the fluid has experienced. In two-dimensional space, plate-like behavior of the lithosphere emerges when the stress induced by the weight of the lithosphere itself is within the range between  $\sigma_D$  and  $\sigma_I$ . Physically, this criterion implies that a plate-like behavior arises only when the mechanical strength of plates (plate margins) is high (low) enough to endure (yield to) the stress induced by the weight of plates themselves.

[6] The Rayleigh number based on reference surface viscosity  $\eta_0^*$  is defined by  $Ra \equiv \rho^* g^* \alpha^* \Delta T^* d^{*3} / \kappa^* \eta_0^*$ , where  $\rho^*$  is density,  $g^*$  is gravitational acceleration,  $\alpha^*$  is thermal expansivity,  $\Delta T^*$  is temperature scale taken to be 2000 K,  $d^*$  is thickness of convecting vessel,  $\kappa^*$  is thermal diffusivity and asterisk stands for dimensional quantities. We fixed  $Ra$  at  $3.0 \times 10^2$ . This  $Ra$  corresponds to  $\eta_0^* = 1.0 \times 10^{26}$  Pa-s. The non-dimensional internal heating rate per unit mass  $Q \equiv \rho^* H^* d^{*2} / k^* \Delta T^*$  is fixed at 10, where  $H^*$  is uniform volumetric internal heating rate per unit volume and  $k^*$  is

thermal conductivity. At this  $Q$ , we found that the internal temperatures are approximately 1. For all cases searched in this study (Table 1), we continue calculations till time-series of averaged quantities such as Nusselt number and root-mean-square (RMS) velocity reach statistically steady states.

[7] The basic equations are discretized by finite volume method on a staggered grid using STAG3D [e.g., *Tackley*, 1996]. The number of mesh points in horizontal and vertical directions are 200 (in both  $x$  and  $y$ -directions) and 64, respectively. The mesh is non-uniform in the vertical direction with higher resolution around the top and bottom boundaries.

### 3. Results

[8] First, we carried out numerical experiments with adiabatic condition on the bottom boundary (Cases A1 to A4 in Table 1). The initial condition employed in Case A1 is  $\omega = 0$  in the entire vessel and the temperature distribution that linearly increases with depth from  $T = 0$  at  $z = 1$  to  $T = 1$  at  $z = 0$ ; a sinusoidal perturbation is superposed to the initial temperature field to start the convection. The initial conditions for Cases A2 to A4 are shown in Table 1.

[9] Figure 2a shows a snapshot of viscosity and velocity distributions on the top surface boundary for Case A1 ( $\Gamma = 50$ ,  $\sigma_I^* = 122$  MPa, and  $\sigma_D^* = 41$  MPa). The RMS velocity on the top surface boundary is at most 10, which corresponds to about 0.01 cm/yr in the dimensional quantity, and  $\omega \ll 1$  on the entire lithosphere. The entire lithosphere is on the intact branch and there is no mechanically weak zones. The convective flow pattern in Case A1 belongs to the “stagnant lid regime” [*Ogawa et al.*, 1991; *Solomatov*, 1995; *Ogawa*, 2003].

[10] When we increased  $\Gamma$  to 400 (Case A3 with  $\sigma_I^* = 43$  MPa and  $\sigma_D^* = 15$  MPa) starting from the temperature- and  $\omega$ -fields obtained at the end of Case A1, in contrast, we

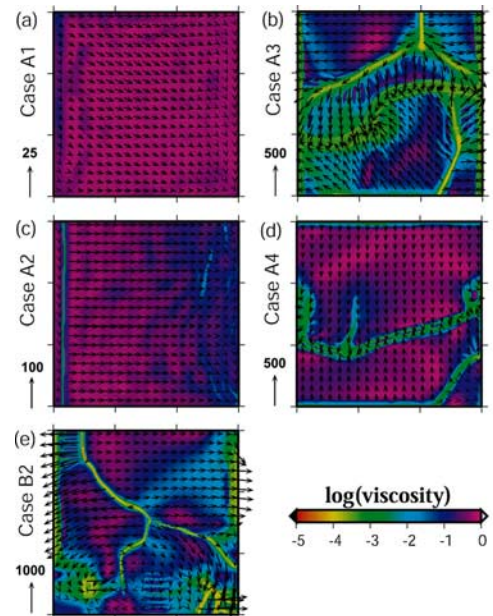


**Figure 2.** Snapshots of the distributions of viscosity (color scale) and horizontal velocity (arrows) on the surface boundary for all of the cases shown in Table 1.

**Table 1.** Summary of the Runs Carried Out in This Study<sup>a</sup>

Case name	$\Gamma$	$\sigma_b^*$	$\sigma_l^*$	IC	PS	Regime
A1	50	41 MPa	122 MPa	(see text)	no	ST
A2	100	29 MPa	86 MPa	Case A1	no	ST
A3	400	15 MPa	43 MPa	Case A1	no	WP
A4	100	29 MPa	86 MPa	Case A3	no	PL
B2	100	29 MPa	86 MPa	Case A2	yes	PL

<sup>a</sup>See Equation (2) for  $\Gamma$ . The stresses  $\sigma_b^*$  and  $\sigma_l^*$  are defined in Figure 1 and Equation (3). The “IC” means the initial conditions and “PS” means the plume seed. The “WP”, “PL” and “ST” in column “Regime” mean the weak plate, the plate-like and the stagnant lid regimes, respectively.

obtained the flow pattern shown in Figure 2b. The lithosphere is divided into several fragments by mechanically weak zones and each fragment moves at the RMS velocity of  $10^2 \sim 10^3$  (0.1 ~ 1 cm/yr). The mechanically weak zones are rather diffuse and we found that the “plateness” defined in *Tackley* [2000b] of the moving plates was around 0.80 at the end of Case A3. We observed that these mechanically weak zones spontaneously developed in the lithosphere when the stress induced by the weight of lithosphere itself exceeded  $\sigma_l$ . This is a feature of the “weak plate regime” defined in *Ogawa* [2003] (see Table 1). Because of the frequent development of new plate margins, the Nusselt number  $\langle Nu \rangle$ , RMS velocity in the entire mantle  $\langle V \rangle$ , and RMS velocity on the top surface boundary  $\langle V_{sur} \rangle$  fluctuate with time as shown in Figure 3.

[11] To understand the nature of convective flow pattern at  $\Gamma$  between 50 adopted in Case A1 and 400 adopted in Case A3, we carried out the numerical experiments of Cases A2 and A4 where  $\Gamma = 100$  (see Table 1). In Case A2, we started the calculation from the outputs obtained at the end of Case A1, which is on the stagnant lid regime (Figure 2c);  $\omega$  is less than 1 even in the linear blue weak zone along the left vertical side wall in Figure 2c and the RMS velocity is still small, around 10 (0.01 cm/yr). When we start the calculation from the outputs obtained at the end of Case A3, which is on the weak plate regime, however, we obtain moving plates as shown in Figure 2d (Case A4). There are well developed mechanically weak zones with  $\omega \gg 1$  and viscosity less than

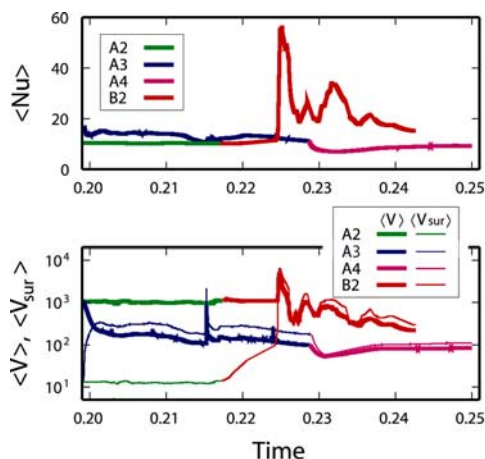


**Figure 3.** Time-series of non-dimensional averaged Nusselt number  $\langle Nu \rangle$  and RMS velocity averaged over the entire mantle  $\langle V \rangle$  and over the top surface  $\langle V_{sur} \rangle$  for Cases A2, A3, A4, and B2.

$10^{-3}$ . We observed that the plateness of the moving plates was around 0.92, much closer to 1 than the plateness of Case A3, when the convective flow was statistically steady. The RMS velocity is around  $10^2$  (0.1 cm/yr) in Case A4, much higher than the average surface velocity obtained in Case A2 (see Figure 3). The fluctuations of  $\langle Nu \rangle$ ,  $\langle V \rangle$  and  $\langle V_{sur} \rangle$  are much smaller in Case A4 than in Case A3. Cases A2 and A4 indicate that the plate-like motion of the lithosphere arises at  $\Gamma = 100$  only when mechanically weak zones are imposed from outside through, say, initial condition. This is a feature of the plate-like regime originally identified for two-dimensional convection [*Ogawa*, 2003]; the plate-like regime exists for three-dimensional convection, too.

[12] Next, we carried out the numerical experiment of Case B2 to see how the lithosphere responds to cylindrical hot uprising plumes on the plate-like regime; hot uprising plumes are found to induce new plate margins on the plate-like regime in two-dimensional space [*Ogawa*, 2003]. Started from the last frame of Case A2 where the lithosphere is stagnant, we superposed a Gaussian-type circular heat flow (“plume seed”) at the center of the bottom boundary; the heat flow on the bottom boundary at  $r^2 \equiv [(x - 1.5)^2 + (y - 1.5)^2] \leq r_p^2$  is  $\partial T / \partial z = f_p \exp(-r^2 / \zeta_p^2)$  where  $f_p$  is fixed at 50,  $r_p$  is 0.50 and  $\zeta_p$  is 0.25. The imposed plume seed at the bottom is kept constant with time during the run. Figure 2e shows a snapshot of distributions of the horizontal velocity and viscosity on the top surface boundary obtained at the end of Case B2. After the plume seed is introduced and an uprising plume reaches the lithosphere ( $t \approx 0.224$ , see Figure 3), the lithosphere is splitted into several fragments by narrow mechanically weak zones and each fragment moves at a significant RMS velocity of around  $3 \times 10^2$  (0.3 cm/yr). The snapshot

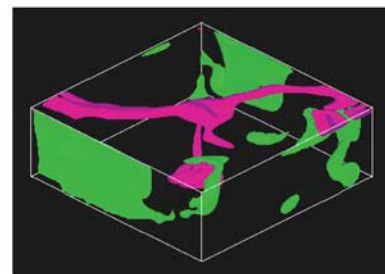


**Figure 4.** Three-dimensional view of thermal structure in the mantle for the convective flow pattern shown in Figure 2e (Case B2). Purple and green iso-surfaces stand for the non-dimensional temperature deviation of +0.15 and -0.15, respectively, from the horizontally averaged temperature at each depths.

of convective flow pattern in Figure 4 shows that downwelling sheet-like cold regions (green parts) extend from the surface to the bottom boundary around the vertical sidewalls of the convecting vessel and linear hot region (purple parts) extends just beneath the spreading center of the lithosphere. Though the hot uprising plume considerably enhances the convective flow at the moment when the plume head breaks the lithosphere, the convective flow soon settles down to its statistically steady state as shown in Figure 3. Cylindrical hot uprising plumes induce new plate margins in three-dimensional space as two-dimensional plumes do on the plate-like regime.

#### 4. Conclusions and Discussion

[13] The three-dimensional numerical model presented here shows that the plate-like regime originally identified for thermal convection in two-dimensional space exists for thermal convection in three-dimensional space, too, when the rheology depends on temperature and stress-history in the way illustrated in Figure 1. The model also shows that cylindrical uprising plumes can newly induce plate margins as mechanically weak zones to maintain stable plate motion on the plate-like regime in three-dimensional space. The plate motions on the plate-like regime presented here (Cases A4 and B2) are as steady as the plate motions induced by yielding and viscosity reduction by melting in the asthenosphere in the earlier three-dimensional models [Tackley, 2000b; Richards *et al.*, 2001] and are much more steady than the plate motions induced by yielding without the help of viscosity reduction by melting [Trompert and Hansen, 1998; Tackley, 2000a]. The stress-history dependence of viscosity induced by the hysteresis illustrated in Figure 1 can induce the stable tectonic-plates in three-dimensional space without the help of viscosity reduction by melting.

[14] Finally, it is interesting to notice that the mechanically weak spreading centers induced by uprising plume observed in Case B2 resembles in shape the triple junctions induced by topographic doming at the initial stage of continental rifting [e.g., Burke and Dewey, 1973]. Formation of new plate boundary by hot uprising plumes may be playing an important role in maintaining the plate motion on the Earth as is the case for the plate-like regime numerically modeled here.

[15] **Acknowledgments.** We are grateful to S. Labrosse and an anonymous reviewer who provided careful reviews. P. J. Tackley kindly provided us with his convection code STAG3D. All the simulations were carried out at the parallel computer systems (SGI origin 2000) of Earthquake Information Center, Earthquake Research Institute, University of Tokyo. M. Y. was financially supported by the Japan Society for the Promotion of Science (JSPS) Research Fellowship. This study was partly supported by the Grand-in-Aid for Scientific Research (JSPS

Fellows, #12-01228) from the Ministry of Education, Culture, Sports, Science and Technology, Japan.

#### References

- Bercovici, D. (1996), Plate generation in a simple model of lithosphere-mantle flow with dynamic self-lubrication, *Earth Planet. Sci. Lett.*, *144*, 41–51.
- Bercovici, D. (1998), Generation of plate tectonics from lithosphere-mantle flow and void-volatile self-lubrication, *Earth Planet. Sci. Lett.*, *154*, 139–151.
- Bercovici, D., and Y. Ricard (2003), Energetics of a two-phase model of lithospheric damage, shear localization and plate boundary formation, *Geophys. J. Int.*, *152*, 581–596.
- Bercovici, D., Y. Ricard, and M. A. Richards (2000), The relation between mantle dynamics and plate tectonics: A primer, in *The History and Dynamics of Global Plate Motions*, *Geophys. Monogr. Ser.*, vol. 121, edited by M. Richards, G. Gordon, and R. D. van der Hilst, pp. 5–46, AGU, Washington, D. C.
- Bercovici, D., Y. Ricard, and G. Schubert (2001), A two-phase model for compaction and damage, 1. General theory, *J. Geophys. Res.*, *106*(B5), 8887–8906.
- Burke, K., and J. F. Dewey (1973), Plume-generated triple junctions: Key indicators in applying plate tectonics to old rocks, *J. Geol.*, *81*, 406–433.
- Christensen, U. (1984), Convection with pressure- and temperature-dependent non-Newtonian rheology, *Geophys. J. R. Astron. Soc.*, *77*, 343–384.
- Moresi, L., and V. Solomatov (1998), Mantle convection with a brittle lithosphere: Thoughts on the global tectonic styles of the Earth and Venus, *Geophys. J. Int.*, *133*, 669–682.
- Ogawa, M. (2003), Plate-like regime of a numerically modeled thermal convection in a fluid with temperature-, pressure-, and stress-history-dependent viscosity, *J. Geophys. Res.*, *108*(B2), 2067, doi:10.1029/2000JB000069.
- Ogawa, M., G. Schubert, and A. Zebib (1991), Numerical simulation of three-dimensional thermal convection in a fluid with strongly temperature-dependent viscosity, *J. Fluid Mech.*, *233*, 299–328.
- Ricard, Y., D. Bercovici, and G. Schubert (2001), A two-phase model for compaction and damage, 2. Applications to compaction, deformation, and the role of interfacial surface tension, *J. Geophys. Res.*, *106*(B5), 8907–8924.
- Richards, M. A., W.-S. Yang, J. R. Baumgardner, and H. P. Bunge (2001), Role of a low-viscosity zone in stabilizing plate tectonics: Implications for comparative terrestrial planetology, *Geochem. Geophys. Geosyst.*, *2*(8), doi:10.1029/2000GC000115.
- Solomatov, V. S. (1995), Scaling of temperature- and stress-dependent viscosity convection, *Phys. Fluids*, *7*, 266–274.
- Tackley, P. J. (1996), Effects of strongly variable viscosity on three-dimensional compressible convection in planetary mantles, *J. Geophys. Res.*, *101*(B2), 3311–3332.
- Tackley, P. J. (2000a), Self-consistent generation of tectonic plates in time-dependent, three-dimensional mantle convection simulations 1. Pseudoplastic yielding, *Geochem. Geophys. Geosyst.*, *1*(8), doi:10.1029/2000GC000036.
- Tackley, P. J. (2000b), Self-consistent generation of tectonic plates in time-dependent, three-dimensional mantle convection simulations 2. Strain weakening and asthenosphere, *Geochem. Geophys. Geosyst.*, *1*(8), doi:10.1029/2000GC000043.
- Trompert, R., and U. Hansen (1998), Mantle convection simulations with rheologies that generate plate-like behavior, *Nature*, *395*, 686–689.
- M. Yoshida, Earth Simulator Center, Japan Marine Science and Technology Center, Showa-machi 3173-25, Kanazawa-ku, Yokohama, Kanagawa 236-0001, Japan. (myoshida@jamstec.go.jp)
- M. Ogawa, Department of Earth Sciences and Astronomy, University of Tokyo, Komaba 3-8-1, Meguro-ku, Tokyo, 153-8902, Japan. (masaki@chianti.c.u-tokyo.ac.jp)